Feruloyl Esterase Fae1 is Required Specifically for Host Colonisation by The Rice-Blast Fungus Magnaporthe Oryzae

Akhil Thaker
The Maharaja Sayajirao University of Baroda Faculty of Science
Khyati Mehta
The Maharaja Sayajirao University of Baroda Faculty of Science
Rajesh Patkar (rajeshpatkar@iitb.ac.in)
Indian Institute of Technology Bombay https://orcid.org/0000-0001-7266-2394

Research Article

Keywords: Ferulic acid, Blast disease, Magnaporthe, Host invasion, Cell wall degradation

Posted Date: June 18th, 2021

DOI: https://doi.org/10.21203/rs.3.rs-591209/v1

Version of Record: A version of this preprint was published at Current Genetics on September 15th, 2021.
See the published version at https://doi.org/10.1007/s00294-021-01213-z.

Feruloyl esterase Fae1 is required specifically for host colonisation by the rice-blast fungus *Magnaporthe oryzae*

Akhil Thaker[1], Khyati Mehta[1], Rajesh Patkar[1,#,*]

[1] *Bharat Chattoo Genome Research Centre, Department of Microbiology and Biotechnology Centre, The Maharaja Sayajirao University of Baroda, Vadodara, Gujarat, India 390002*

[#] *Present address: Department of Biosciences and Bioengineering, Indian Institute of Technology Bombay, Powai, Mumbai, Maharashtra, India 400076*

[*] Author for correspondence – Rajesh Patkar - rajeshpatkar@iitb.ac.in

Key words: Ferulic acid; Blast disease; Magnaporthe; Host invasion; Cell wall degradation

Abstract

Plant cell wall acts as a primary barrier for microbial pathogens during infection. A cell wall degrading enzyme thus may be a crucial virulence factor, as it may aid the pathogen in successful host invasion. Nine genes coding for feruloyl esterases (Fae), likely involved in plant cell wall degradation, have been annotated in the genome of the cereal-blast fungus *Magnaporthe oryzae*. However, role of any Fae in pathogenicity of *M. oryzae* remains hitherto under explored. Here, we identified *FAE1* gene (MGG_08737) that was significantly upregulated during host penetration and subsequent colonisation stages of infection. Accordingly, while deletion of *FAE1* in *M. oryzae* did not affect the vegetative growth and asexual development, the *fae1*Δ mutant showed significantly reduced pathogenesis on rice plants, mainly due to impaired host invasion and colonisation. Very few (<10%) *fae1*Δ appressoria that formed the primary invasive hyphae, failed to elaborate from the first invaded cell to the neighboring plant cells. Interestingly, exogenously added glucose, as a simple carbon source, or ferulic acid, a product of the Fae activity, significantly supported the invasive growth of the *fae1*Δ mutant. We show that the Fae1-based feruloyl esterase activity, by targeting the plant cell wall, plays an important role in accumulating ferulic acid and/or sugar molecules, as a likely energy source, to enable host invasion and colonisation by *M. oryzae*. Given its role in plant cell wall digestion and host colonisation, *M. oryzae* Fae1 could be a potential candidate for a novel antifungal strategy and a biotechnological application in biofuel production.

Introduction

Microbial phytopathogens encounter plant cell wall as a major obstruction while invading and successfully colonizing the host. Typical plant cell wall is primarily composed of three polysaccharides namely cellulose (microfibrils), hemicellulose (xylan and xylan derivatives) and pectin, interconnected via ferulic acid bridges to form a rigid mesh-like structure (Harris and Hartley, 1977; Bunzel et al., 2001). This mesh-like network is required for providing strength and integrity to the plant cell wall. Phytopathogens, such as fungi and bacteria, deploy different ways to overcome this physical cell wall barrier, mainly to get entry into the host cell and colonise the tissue for nutrient acquisition. While bacterial pathogens prefer passive host entry via hydathodes or stomatal openings, fungal pathogens have evolved mechanisms to breach the primary barrier of plant hosts. The necrotrophic fungal pathogens use cell wall degrading enzymes (CWDE) to invade/colonise the plant tissue (Cosgrove, 2001); whereas the biotrophic or hemibiotrophic fungal pathogens, in addition to CWDE, depend on specialised host entry enabled by infection structures called as appressorium (Howard et al., 1991). While, CWDEs are fairly studied with respect to virulence of phytopathogenic fungi, they are also implemented in industrial applications such as processing of plant cell walls for efficient production of biofuels. Ever-increasing collection of genome sequences reveals that CWDEs offer a wide diversity, both in terms of number and expansion of gene families, across phytopathogenic fungi (Kubicek et al., 2014). It is therefore important to study different CWDEs, which may lead to identification of novel virulence determinants in different phytopathogenic fungi.

Feruloyl esterases (Ferulic acid esterases, Fae; EC 3.1.1.73), a subclass of carboxylic acid esterases (EC 3.1.1.1), also belong to one such group of CWDEs. The Fae hydrolyses the ester bonds in the feruloyl-polysaccharide complex in the plant cell wall and thereby releases ferulic acid and polysaccharide (Faulds and Williamson, 1994; de Vries et al., 1997).

Breakage of these ester bonds leads to loss of elasticity and plasticity and subsequent weakening of the plant cell wall. Feruloyl esterases have been classified into four classes - type A, B, C and D - depending upon sequence attributes and ability to act on wide range of substrates (Crepin et al., 2004). Crystal structure of feruloyl esterase from *Aspergillus niger* (AnFaeA) has revealed that it is a modular enzyme with a catalytic and a non-catalytic cellulose-binding domain (Hermoso et al., 2004). Involvement of fungal feruloyl esterases with differential activity during plant infection have been studied in different pathosystems. In *Fusarium graminearum*, feruloyl esterases, particularly FaeB1 and FaeD1, are found to be upregulated during infection or in response to aromatic compounds such as ferulic acid, caffeic acid and p-coumaric acid and also in the presence of carbon sources such as xylose, glucose and galactose (Balcerzak et al., 2012). However, FaeB1 and FaeD1 are not required for pathogenicity on wheat (Balcerzak et al., 2012). On the other hand, expression of Fae is not only upregulated during infection but also plays an essential role in pathogenesis in the apple tree canker pathogen *Valsa mali* (Xu et al., 2017).

Magnaporthe oryzae, a hemibiotrophic phytopathogenic filamentous fungus, causes blast disease in rice and other important cereal crops worldwide (Valent and Khang, 2010). Over several years, rice-blast disease has been widely used as a model pathosystem to study plant-pathogen interactions (Ebbole, 2007; Patkar et al., 2015). The infection cycle of *M. oryzae* starts with conidial germination in the presence of moisture, followed by perception of specific cues from the host surface, leading to development of appressorium. The enormous turgor pressure generated inside the appressorium helps the fungus in penetrating the host cell. While the intracellular turgor pressure inside the appressorium contributes in generating the mechanical force, the localised loosening of the host cell wall underneath the appressorium is important and carried out by certain plant cell wall digesting enzymes secreted by the fungal pathogen. During subsequent host tissue invasion, the penetration peg

differentiates into bulbous primary invasive hypha that elaborates within the first invaded cell. Once inside the first host cell, the fungal pathogen uses different strategies to evade plant immunity to colonise the tissue and for disease progression (Skamnioti and Gurr, 2008; Patkar et al., 2015).

Role of CWDEs in host penetration and thereby virulence has been studied in *M. oryzae*. Endo-xylanases and cellulases are significantly upregulated during plant infection and required for penetration and virulence in *M. oryzae* (Nguyen et al., 2011; Vu et al., 2012). Further, a secreted feruloyl esterase A, encoded by MGG_01403.5, in *M. oryzae* is found to be expressed during post-penetration stage (72 hpi onwards) of rice infection, but does not play a significant role in pathogenesis of the fungus (Zheng et al., 2009). Interestingly, the *FAE* gene family in *M. oryzae* is relatively expanded when compared to that in non-pathogenic counterparts such as *Neurospora crassa* and *Aspergillus nidulans*, which have only one and three *FAE* genes, respectively (Dean et al., 2005). Hitherto, role of any other *FAEs* has not been studied in *M. oryzae*. Here, we studied the expression profiles of nine *FAE* genes, to identify an early invasion-related Fae function. We show a crucial role for one of the Fae, in host invasion and tissue colonisation. Our *in silico* analysis of these Fae also highlights a likely diversification of the sequences in a host-specific manner.

Experimental Procedures

Fungal culture and growth conditions

M. oryzae wild-type (WT) B157 strain (MTCC accession no. 12236; Kachroo et al., 1994) belonging to the international race IC9 was used in this study. Fungus was grown and maintained on Prune Agar (PA) plates as described earlier (Soundararajan et al., 2004).

Vegetative growth of the fungus on PA plates was allowed for 10 days at 28 °C, with initial 3 days incubation under dark conditions followed by 7 days incubation under constant illumination for conidiation. Vegetative growth was assessed by visual observation of the colony morphology and by measuring the colony diameter. Conidia were harvested as described previously (Patkar et al., 2010), followed by microscopic observation of the conidial morphology. Harvested conidia were counted using a hemocytometer and reported in terms of total number of conidia per unit area of the colony.

Assay for appressorial development was performed by spotting 20 µL conidial suspension (~10^4 conidia/mL) on an inductive (hydrophobic) cover glass (22 mm, no. 1; Microcil Ltd., India) for up to 24 hours at 25 °C under humid conditions, followed by assessment of appressorium formation by microscopic observation.

Nucleic acids and proteins were isolated by grinding in liquid nitrogen the fungal biomass obtained from vegetative culture grown in an appropriate liquid medium for 2 – 3 days at 28 °C, followed by the standard protocols mentioned earlier (Dellaporta et al., 1983; Kachroo et al., 1997).

Identification and *in silico* analysis of fungal *FAE*s

Initial identification of putative feruloyl esterases in *M. oryzae* was done using NCBI protein BLAST (https://blast.ncbi.nlm.nih.gov/Blast.cgi?PAGE=Proteins) with known Fae sequences from *Aspergillus oryzae* (AoFaeB; PDB: 3WMT_B) and *Neurospora crassa* (NcFaeB; GenBank: AJ293029). Multiple sequence alignment of these putative Fae was carried out using ClustalW feature in MEGA tool to check the presence of GXSXG conserved motif (Dilokpimol et al., 2016). Presence of the characteristic α/β hydrolase domain was checked

using the NCBI conserved domain database (http://www.ncbi.nlm.nih.gov/Structure/cdd/wrpsb.cgi; Marchler-Bauer et al., 2015). Further, percentage identity among all these *M. oryzae* Fae was checked by performing multiple sequence alignment of protein sequences using Clustal Omega (Sievers et al., 2011; Sievers and Higgins, 2018), followed by plotting the distance matrix heatmap using R tool (Supplementary Fig. S5).

Phylogenetic analysis of Fae in different host-specific isolates of *M. oryzae* (GY11, P131, Y34, PH14, US71, MZ5-1-6, CD156, BR32) was carried out using the annotated protein sequences, available in the NCBI and GEMO (http://genome.jouy.inra.fr/gemo/) databases, from these isolates. Protein sequences of putative Fae in *M. oryzae* 70-15 strain was used as a query to perform BlastP analysis with a custom database containing all the protein sequences from the aforementioned different isolates. Phylogenetic analyses were carried out with MEGA7 (Kumar et al., 2016), using the Maximum Likelihood method based on the JTT matrix-based model.

For phylogenetic analysis of feruloyl esterases across different fungal taxa, genome sequences of 21 representative fungal species (Table S1) were retrieved from the NCBI database. Proteomes were mined for the presence of the conserved domain Tannase (Pfam ID: PF07519) or Esterase_PHB (Pfam ID: PF10503), using hmm-search (hidden Markov model-search) of HMMER suite (parameters -cut_tc; Hancock & Bishop, 2004). Poorly aligned sequences were removed using TrimAl (Capella-Gutierrez et al., 2009; parameters -automated1). Alignment of Tannase domain containing sequences was used to construct the maximum likelihood phylogenetic tree, using IQ-TREE (Nguyen et al., 2015). Firstly, best fit model (LG+I+G4) was chosen based on the Bayesian Information criterion (BIC), followed by assessment of phylogenetic tree for branch support with ultrafast bootstrap (parameters -m

model -alrt 1000 -bb 1000 -nt AUTO). Phylogenetic tree was visualized using iTOL (Letunic and Bork, 2019).

Signal peptide prediction and validation

Prediction of conventional secretory signal peptide was carried out using SignalP 4.0 tool (http://www.cbs.dtu.dk/services/SignalP-4.0/; Petersen et al., 2011). Presence of functional signal peptide was confirmed for two randomly selected *FAE*s - MGG_05529 and MGG_07294 - using Yeast Secretion Trap (YST) approach as described (Lee et al., 2006). The ORFs of MGG_05529 and MGG_07294 were PCR-amplified from *M. oryzae* WT genomic DNA, using the following primer pairs (MGG_05529-F: 5'-ATGGACTCGTCAATCATTCACTGG-3' and MGG_05529-R: 5'-CCCCATTCCACTTTGACCTG-3'; MGG_07294-F: 5'-ATGCGTTTCTCCAGCATCTTC-3' and MGG_07294-R: 5'- CGCAATGAGACCAAAGAACC-3'). Individual PCR products were subjected to blunt end cloning in pYST2 vector at *Not*I site after end-filling, followed by *E. coli* DH5α transformation. Transformants obtained on Luria-agar plates containing 100 µg/mL ampicillin antibiotic were screened by RE digestion and those with desired restriction digestion pattern were confirmed by DNA sequencing. These recombinant plasmids from desired clones of *E. coli* DH5α were used for yeast (*Saccharomyces cerevisiae*) DBYα2445 (MATα, *suc2*Δ*–9*, *lys2–801*, *ura3–52*, *ade2–101*) transformation as described previously (Gietz and Woods, 2002). Selected transformants were screened and confirmed by colony PCR. Confirmed *S. cerevisiae* transformants were spotted on SD (YNB with $(NH_4)_2SO_4$, Lysine, Uracil and Adenine) + sucrose agar selection plates and incubated for 6 days at 28 °C.

Determination of fungal Fae activity

In order to check the effect of host-extract on Fae enzyme activity, 3-day-old vegetative culture of WT *M. oryzae* grown in liquid YEG (0.2% Yeast-extract and 1% glucose) medium with or without crude rice leaf extract was used. Protein samples were prepared from fungal biomass (intracellular proteins) and culture supernatant (secretory proteins), essentially as described earlier (Kachroo et al., 1997), followed by biochemical spectrophotometric enzyme assay using Fae-specific substrate, 4-nitrophenyl ferulate (Institute of Chemistry, Slovak Academy of Sciences, Bratislava), as described previously (Mastihuba et al., 2002). Protein estimation was carried out using Bradford reagent and standard curve method (B6916; Sigma-aldrich, USA). Finally, specific activity (mU mg^{-1}) of Fae was calculated for intracellular and secretory protein fractions from both control and rice-extract-treated samples.

Gene expression analysis by qRT-PCR

For gene expression analysis under host- or pathogenicity-mimic conditions, 3-day old vegetative culture of WT *M. oryzae* grown in liquid complete medium (CM; 0.5% Peptone, 0.1% Yeast-extract, 0.1% CAA, 0.05% KCl, 0.05% $MgSO_4$, 0.15% KH_2PO_4, 1% glucose, 0.6% $NaNO_3$; pH 6.5) was used. Fungal biomass was harvested and washed thrice with sterile distilled water followed by aseptic transfer in nearly equal amounts to the following seven different media conditions: 1) Minimal medium (MM; 0.05% KCl, 0.05% $MgSO_4$, 0.15% KH_2PO_4, 1% glucose, 0.6% $NaNO_3$; pH 6.5) as a control condition, 2) MM (w/o glucose) + 0.03% cutin monomers (1,16-hexadecanediol; Sigma); 3) MM (w/o glucose) + 0.03% ferulic acid (Sigma); 4) MM minus $NaNO_3$ (nitrogen starvation); 5) MM (w/o glucose) + 1% pectin (Sigma); 6) MM (w/o glucose) + 1% N-acetylglucosamine (NAG;

189 HiMedia) and 7) MM (w/o glucose) + 1% xylan (Sigma). Fungal cultures were then treated
190 in aforementioned media conditions for 48 hours under shaking conditions at 28 °C, followed
191 by qRT-PCR analysis.

192 Similarly, *FAE*s gene expression profile during different stages of infection (*in vivo*) was
193 studied using a method, with modifications, reported earlier (Skamnioti and Gurr, 2007).
194 Briefly, a 15-20 µL WT conidial suspension (~10^5 conidia/mL; containing 0.05% gelatin)
195 was drop-inoculated on the surface-sterilized 2 – 3-week old barley leaf blades placed on to
196 kinetin-agar plates, followed by incubation under dark (8 h) and light (14 h) cycles at 25 °C.
197 Samples for RNA extraction were collected by excising inoculated portion of the leaf blades
198 at different time-points viz. 12, 24, 48, 72- and 96-hours post inoculation (hpi) along with 3-
199 day old vegetative mycelia, grown in liquid CM, as a control condition for qRT-PCR
200 analysis. A sample from mock-inoculation i.e., leaves inoculated with only 0.05% gelatin
201 solution, was used as a negative control for any non-specific amplification during qRT-PCR.

202 Total RNA was extracted from the samples collected for each of the above-mentioned
203 conditions/time-points using TRIzol® reagent (Invitrogen, USA), as per the manufacturer's
204 instructions. A total of 2 µg of total RNA each was used for the first strand cDNA synthesis
205 using Oligo-$(dT)_{18}$ primers (Sigma, India) and M-MuLV reverse transcriptase (New England
206 BioLabs, USA). The first strand cDNA was then subjected to qRT-PCR analysis using a
207 Power SYBR® Green PCR Master Mix (Applied Biosystems, USA), performed on a 7900HT
208 Fast Real-Time PCR System (Applied Biosystems, USA) according to the manufacturer's
209 instructions. Optimized thermal cycling conditions for qRT-PCR were as follows: initial
210 denaturation step at 95 °C for 15 minutes followed by 40 cycling reactions each at 95 °C
211 (denaturation step) for 15 seconds and 66 °C (annealing and extension step) for 45 seconds.
212 Transcript levels in each of the test conditions were calculated by $2^{-\Delta\Delta Ct}$ method (Livak
213 method; Livak and Schmittgen, 2001) relative to that of the vegetative mycelia grown in

liquid MM or CM, normalized against β-tubulin (MGG_00604) transcript levels as an endogenous (loading) control. Primers used for qRT-PCR analysis are listed in the Table S2.

Generation of *FAE1* deletion mutant and genetic complementation of *fae1*Δ strain

FAE1 gene (Gene ID: MGG_08737) deletion construct was made by double-joint PCR approach (Yu et al., 2004) using hygromycin phosphotransferase (*HPT*) gene as a selectable marker, followed by targeted gene replacement in WT *M. oryzae* via homologous recombination (Supplementary Fig. S1A). Here, ~1 kb each of 5' and 3'-untranslated regions (UTR) of *FAE1* gene were amplified from WT genomic DNA and fused with *HPT* gene cassette, using a recombinant PCR, followed by another round of PCR with nested primers to get a specific amplification product (Table S3). This recombinant PCR product was further purified by Na-acetate/ethanol precipitation and used for polyethylene glycol (PEG)-mediated fungal transformation (Prakash et al., 2016), using WT *M. oryzae* protoplasts. Fungal transformants were selected on YEG agar plates containing 200 µg/mL hygromycin. Transformants growing on the selection medium were further screened by locus-specific PCR, where only one out of a total 72 transformants showed the desired amplified PCR product (Supplementary Fig. S1B). This transformant was further analysed by RT-PCR, wherein, as expected, no transcript was detected when compared with the WT or an ectopic transformant (Supplementary Fig. S1C).

Next, the selected transformant was confirmed for site-specific integration (replacement of the *FAE1* ORF with the selectable marker gene) by Southern blot hybridization. Genomic DNA was extracted from the WT and *fae1*Δ strains and further subjected to restriction enzyme digestion with *Pst*I. The *HPT* gene, used as a probe, was labeled and DNA detection was performed using Alkphos Direct labeling and detection kit (GE Healthcare Ltd., UK)

following the manufacturer's instructions. Southern blot hybridization analysis confirmed replacement of the *FAE1* ORF in the mutant with a single copy of *HPT* gene cassette (Supplementary Fig. S1D).

For genetic complementation of *fae1*Δ strain, a full-length genomic sequence of *M. oryzae* *FAE1* ORF (MGG_08737) along with 5'-UTR (~ 1.5 kb) was amplified by PCR using FAE-8737-5'UTR(F) and FAE-8737-NST(R) primers (Table S4). The amplified PCR product was cloned at *EcoR*I/*Xba*I sites in pFGL889-*ILV2*^{SUR} based pFGL1010 vector (Yang and Naqvi, 2014; Addgene plasmid # 119081). The cloned 5'UTR-*FAE1* ORF sequence was confirmed by restriction enzyme digestion of the recombinant plasmid pRPL049. Further, the final sequence for complementation was PCR-amplified from the pRPL049 recombinant plasmid using LB-F1 (5'-TGCGGACGTTTTTAATGTACTG-3') and RB-R1 (5'-GAAACGACAATCTGATCCAAGC-3') primers. The amplified PCR product was again confirmed by restriction enzyme digestion and purified by gel extraction (QIAEX® II Kit, Qiagen, Germany), and subsequently introduced into *fae1*Δ strain by protoplast transformation (Prakash et al., 2016). As described previously (Yang and Naqvi, 2014), the transformants were selected on Basal Medium (BM) containing 100 µg/mL chlorimuron ethyl, as only those with *ILV2*^{SUR}-5'UTR-*FAE1* integrated at the native *ILV2* locus will be able to grow on this selection medium. Chlorimuron ethyl resistant transformant was then confirmed by locus-specific PCR using ILV2-5'UTR (5'- TTGTCATCGTCTGACAGGTC) and FAE-8737-5'UTR-R (Table S4) primers and further analysed by RT-PCR, wherein *FAE1* transcript could be detected (Fig S1E and S1F).

Whole-plant infection and *in vitro* host-invasion assays

Whole-plant infection assay was carried out by spraying ~10^5 conidia/mL in 0.05% w/v gelatin onto ~4-week old rice plants, followed by incubation at 28 to 30°C under humid conditions, initially for 24 h in the dark and then for 4 to 6 days under 14 h light and 10 h dark cycles. Development of disease symptoms was monitored regularly during the entire incubation period and recorded at an appropriate time.

Host invasion by the fungal strains was checked by inoculating ~20 µL conidial suspension (~10^4 conidia/mL) on to the leaf sheaths obtained from 3 – 4-week old host (rice, wheat or barley) plants, followed by incubation at room temperature (<30 °C) under humid conditions. Host invasion was observed and quantified by scoring at least 100 appressoria each, using bright-field microscopy (Olympus BX51, Japan), for the development of invasive hypha in the plant cell underneath, at ~48 or 96 hpi. To check the effect of exogenous supply of glucose (2% w/v), ferulic acid (100 mM) or reduced glutathione (GSH, 20 mM) on host invasion by the blast fungus, the compound was added to the rice leaf sheaths, already inoculated with conidia, at 22 hpi, and the resultant invasive hyphal growth was observed at ~48 hpi.

Statistical analyses

Quantitative analyses for fungal Fae enzyme activity, transcript levels, vegetative growth, conidiation, appressorial development and host-invasion ability were carried out with three independent sets and the results are reported as mean ± standard deviation of mean (SDM). Statistical significance was determined by using two-tailed *t*-test; and *P*-values less than 0.05 (i.e. < 5%) were considered as statistically significant. $P < 0.05$ is denoted as * and likewise $P < 0.01$ as ** and $P < 0.001$ as ***.

Results

Identification and *in silico* analysis of feruloyl esterase (*FAE*) gene(s) in *M. oryzae*

We performed a protein BLAST analysis using the known Fae sequences from *Aspergillus oryzae* (AoFaeB; PDB: 3WMT_B) and *Neurospora crassa* (NcFaeB; GenBank: AJ293029) as a query against *M. oryzae* 70-15 reference genome database. We found in *M. oryzae* genome a total of nine putative feruloyl esterases that showed homology with either AoFaeB or NcFaeB. While MGG_08737 and MGG_07294 showed highest (47% and 75%) identity to AoFaeB and NcFaeB, respectively (Table S2), MGG_03771 showed similarity to both the reference sequences. Feruloyl esterases belong to the α/β-hydrolase-fold superfamily and catalyze substrate hydrolysis following the mechanism of serine proteases with a conserved GXSXG motif and Ser-His-Asp/Glu catalytic triad (Dilokpimol et al., 2016). Our multiple sequence alignment of all nine putative Fae in *M. oryzae* showed the presence of the conserved GXSXG motif (Fig. 1A).

Next, we performed an hmm-based search for the presence of Tannase (Pfam ID: PF07519) or Esterase_PHB (Pfam ID: PF10503) domain, another characteristic of Fae, within the protein sequences of twenty-one representative fungi, including *M. oryzae* (70-15), belonging to seven different taxonomic classes. We found in these fungi a total of 203 putative Fae protein sequences, of which 151 showed presence of Tannase domain, whereas the remaining 52 protein sequences contained an Esterase_PHB domain (Table S1). Here, the *M. oryzae* genome, unlike in the aforementioned GXSXG motif-based analysis, showed twelve putative Fae sequences, wherein nine contained Tannase and the rest three had Esterase_PHB domain.

Interestingly, majority of the phytopathogenic fungi such as *Fusarium spp.*, *V. mali*, *Magnaporthe spp*., *Colletotrichum graminicola* and *Zymoseptoria tritici* showed more than one, Tannase domain containing, highly variable Fae sequences. However, *Ustilago maydis*, a basiodiomycete causal agent of corn smut disease, showed only one Esterase_PHB and zero Tannase domain containing Fae sequence. Intriguingly, the non-pathogenic filamentous fungi such as *N. crassa*, and particularly *Aspergillus spp.*, also showed more than one putative *FAE* in their genomes; whereas, fission yeast (*S. pombe*) or budding yeast (*S. cerevisiae*) did not show any Fae sequence.

Further, we analysed the phylogenetic relationship of all the putative Fae, containing Tannase domain, in the aforementioned fungal species. The phylogenetic tree showed that Fae sequences had a significant genetic diversity and a discontinuous distribution pattern even among multiple Fae of the same species (Fig. 1B). Out of the nine Tannase domain containing *M. oryzae* Fae (MGG_03771, MGG_03502, MGG_05366, MGG_02261, MGG_05592, MGG_08737, MGG_09404, MGG_09677 and MGG_09732), MGG_08737 (depicted as filled-star in Fig.1B) seemed to be highly diverged and is grouped into a sub-clade exclusive to *Magnaporthales* order.

We then performed, using MEGA tool, a phylogenetic analysis of combined sequences of Fae from a few host-specific strains of the blast fungal pathogen isolated from various cereal crops such as rice, wheat and millet (Fig. 1C and Supplementary Fig. S2). Interestingly, our analysis showed divergence of feruloyl esterase genes, especially MGG_9404 and MGG_08737, in a host-specific manner (Fig. 1C and Supplementary Fig. S2), suggesting a crucial function for these sequences in pathogenesis likely towards distinct hosts.

M. oryzae Fae are induced in the presence of host extract and are secretory in nature

We presumed that *M. oryzae* Fae would be required to function outside the cell; and hence studied whether these fungal enzymes were secretory in nature. Firstly, we checked the presence or absence of a secretory signal peptide in the amino acid sequences of the aforementioned nine Fae using SignalP program. We found that a conventional secretory signal peptide was present in seven out of nine Fae in *M. oryzae* (Table S2). In order to validate this observation, two putative *FAE* genes were randomly selected and subjected to the Yeast Secretion Trap (YST) system as described earlier (Fig. 2A; Lee et al., 2006). The two *FAE* genes (MGG_05529 and MGG_07294) were then individually cloned in-frame, in the vector pYST2, with the *SUC2* invertase gene without its native signal peptide, and transferred individually to the budding yeast (*S. cerevisiae*) strain DBYα2445, which does not carry its native *SUC2* invertase gene. Thus, neither the untransformed yeast strain nor a transformant with the backbone vector would be able to grow on selection medium containing sucrose as the sole carbon source. However, the yeast transformant expressing the Suc2 fused with Fae would be able to utilize sucrose in the selection medium, only if a signal peptide on Fae aids in secretion of the invertase. Indeed, the yeast transformants harboring the plasmid with Suc2 fused to either of the two *FAE* genes grew on sucrose agar, confirming the presence of a signal peptide and thereby the secretory nature of Fae enzymes in *M. oryzae* (Fig. 2B).

Next, to check whether the host tissue had any effect on *M. oryzae* Fae activity, the WT fungal culture was grown in YEG broth with or without crude rice leaf extract. Both, fungal biomass and culture supernatant, were collected separately and subjected to the *in vitro* enzyme activity assay. We found that the total enzyme activity was significantly higher (166 ± 3.33 mU mg^{-1}; $P < 0.001$) in the extracellular (secretory) fraction of the culture grown in the presence of rice leaf extract, when compared with that (29 ± 0.69 mU mg^{-1}) without the host extract (Fig. 2C). Importantly, the total enzyme activity in the intracellular fraction was

less and remained largely unchanged even in the presence of the host leaf extract (Fig. 2C). These results indicate that most *M. oryzae* Fae are secretory and that their expression is induced by the host-derived factors suggesting a likely role for the CWDE in blast fungal pathogenesis.

M. oryzae Fae express differentially during pathogenesis

Given that the CWDEs are expressed under tight regulation (Zheng et al., 2009) and that *M. oryzae* Fae secretion was induced in the presence of rice leaf extract, we studied accumulation of nine *FAE* transcripts in response to individual host cell wall components. Considering the relatively higher turnover of the plant cell wall components during infection, we grew the vegetative culture in media containing - 1) Ferulic acid, 2) Pectin, 3) Xylan, 4) N-acetyl glucosamine (NAG; fungal cell wall component), 5) Cutin monomer (inducer of appressorial development), 6) Nitrogen starvation (mimic of pathogenic development) or 7) Glucose (control condition). Intriguingly, while there was no obvious pattern in accumulation of any particular transcript in response to the plant cell wall components, majority of the *FAE*s showed a ≥2-fold increase in expression in the presence of NAG (Fig. 3A). Whereas, those of almost all the *FAE*s were significantly lowered, either due to N_2 starvation or in the presence of xylan (Fig. 3A). Our findings suggest that the expression of *M. oryzae FAE* could be induced by likely activity of plant or fungal chitinase during the host-pathogen interaction.

Next, we studied the expression of *FAE*s during both pre- and post-host-invasion. The WT conidia were inoculated on detached barley leaves and samples were harvested at specific time-points signifying different stages of blast fungal infection cycle - pre-invasive appressorial development (12 h), host penetration and colonisation (24-48 h) followed by necrotrophic growth phase (48-96 h). The relative transcript levels of all the nine *FAE*s were

estimated by qRT-PCR during aforementioned infection stages and compared with those from the vegetative mycelia grown in liquid complete medium. While, almost all the *FAE* genes showed differential upregulation at different phases of pathogenic life cycle, remarkably, MGG_08737, hereafter referred as *FAE1*, showed a significant increase in relative transcript levels (~300-fold) during pre-invasive appressorial development and host penetration stages (12 and 24 hpi) when compared to those of the other *FAE*s from the vegetative mycelia (Fig. 3B). The *FAE1* transcript levels further increased (~470-fold) during the subsequent host colonisation (48 hpi) and remained at elevated level (~293-fold) at 72 hpi, followed by a sharp decline (~27-fold) at 96 hpi (Fig. 3B). Importantly, the *FAE1* transcript profile here is in accordance with the global transcriptome reported earlier in *M. oryzae* (Jeon et al., 2020). Our observations indicate that feruloyl esterases, particularly Fae1, has an important role during pathogenesis in the blast fungal pathogen.

M. oryzae Fae1 function is required specifically for host invasion

Given the significant upregulation of *FAE1* during pre- and post-invasion, we generated a *fae1*Δ mutant to study its role, if any, in fungal development and pathogenesis. We first studied different phenotypic characteristics, such as vegetative mycelial growth and asexual (conidial) development, of the *fae1*Δ mutant. The vegetative growth of the *fae1*Δ mutant, after 10 dpi, was comparable to that of the WT, where colony size, morphology and melanization on PA plates was similar in both the strains (Fig. 4A). While, the colony diameter of the WT was 7.37 ± 0.06 cm that of the *fae1*Δ was 7.17 ± 0.06 cm (Fig. 4B). Further, total conidiation was determined by harvesting asexual conidia from vegetative culture on PA plates at 10 dpi. The *fae1*Δ produced 102.2 ± 12.2 $\times 10^2$ conidia/cm^2 that was comparable to the 99.1 ± 7.4 $\times$ 10^2 conidia/cm^2 produced by the WT (Fig. 4C).

Given a significant increase in the *FAE1* transcript levels also at the pre-invasive stage (12 hpi), we studied appressorial development in the *fae1*Δ mutant. Appressorial assay carried out on an artificial hydrophobic surface showed that the morphology of the *fae1*Δ appressoria was comparable to that of the WT appressoria observed at 24 hpi (Fig. 4D). We further quantified the appressorial development and found that the % appressoria formed was similar in both the WT (83.0 ± 1.5 %) and *fae1*Δ mutant (81.7 ± 0.82 %) (Fig. 4E). These results indicate that Fae1 does not play an important role in vegetative growth, asexual development and host-independent early pathogenic development in *M. oryzae*.

Next, we tested the pathogenicity of the *fae1*Δ mutant on the host, where rice or barley whole plants were spray-inoculated with conidia harvested from the WT, *fae1* Δ or *fae1*Δ/*FAE1* strain and incubated under humid conditions for 5-6 days. Interestingly, the *fae1*Δ-inoculated plants did not show typical blast disease lesions indicating that the mutant was significantly reduced in pathogenesis when compared with the WT or *fae1*Δ/*FAE1* strain (Fig. 5A and Supplementary Fig. S4A).

To further investigate the impaired pathogenesis in the *fae1*Δ strain, we studied the invasive growth, if any, of the mutant by microscopically observing the rice sheath inoculated with the WT or mutant. We found that most *fae1*Δ appressoria were unable to form visible primary invasive hyphae in rice sheath tissue (Fig. 5B). While 77.33 ± 5.41% and 56.88 ± 2.29% of the WT and *fae1*Δ/*FAE1* appressoria, respectively, formed clearly visible invasive hyphae, only 3.28 ± 0.25% *fae1*Δ appressoria were able to invade and form primary invasive hyphae ($P < 0.001$; Fig. 5C). Further, importantly, the primary invasive hyphae formed by the *fae1*Δ mutant were restricted in the first invaded host cell and failed to elaborate to the neighboring cells (Fig. 5B). In order to rule out the possibility of delayed colonisation by the *fae1*Δ mutant, we checked the invasive growth at 96 hpi. Indeed, even after prolonged incubation,

the *fae1*Δ mutant failed to colonize the plant tissue, as opposed to profuse invasive hyphal growth of the WT by then (Supplementary Fig. S3A). Similar phenotypes were also observed for the *fae1*Δ mutant on other host plants such as barley and wheat (Supplementary Fig. S4B and S4C). Given that the Fae activity on the plant cell wall would release ferulic acid and polysaccharide molecules, we wondered whether exogenous supply of these compounds would support the *fae1*Δ mutant in efficient host tissue colonisation. We performed an *in vitro* host-invasion assay on rice sheath inoculated with *fae1*Δ mutant with 2% glucose or 100 mM ferulic acid, added at 22 hpi (just before the onset of host penetration), and observed at ~48 hpi (Fig. 5B and Supplementary Fig. S3B). Indeed, while exogenously supplied glucose significantly rescued the *fae1*Δ strain, addition of ferulic acid moderately (42.9 ± 4.6 %; $P < 0.001$) restored the host invasion and colonisation ability in the mutant (Fig. 5C). This observation was further substantiated by the whole-plant infection assay wherein the rice plants inoculated with the *fae1*Δ mutant showed development of disease lesions upon exogenous addition of glucose or ferulic acid (Fig. 5B). To find out whether ferulic acid served as an antioxidant, we inoculated both leaf and sheath tissues with the *fae1*Δ mutant in the presence of 20 mM GSH, which is a known antioxidant. However, unlike ferulic acid, exogenous addition of GSH could not rescue the *fae1*Δ mutant (Fig. 6A and 6B). Hence, we wondered whether *M. oryzae* could utilize ferulic acid as an energy source, since often small phenolic compounds such as ferulic acid can be used by fungi as an alternative or weak energy source (Black and Dix, 1976). Indeed, we found that *M. oryzae* WT grew on the basal medium supplemented with ferulic acid as the sole carbon source (Fig. 6C). This also possibly explains how exogenous addition of ferulic acid could rescue the *fae1*Δ strain, most likely by providing energy to support invasive growth rather than acting as an antioxidant.

Altogether, our results show that the Fae1-based likely plant cell wall degradation is required specifically for successful host-invasion and colonisation during pathogenesis in *M. oryzae*.

Discussion

Plant cell wall degrading enzymes (CWDEs) play a pivotal role in virulence of phytopathogenic fungi. Feruloyl esterases belong to α/β-hydrolase-fold superfamily and catalyze substrate hydrolysis following the mechanism of serine proteases having a conserved motif GXSXG and a conserved Ser-His-Asp/Glu catalytic triad (Dilokpimol et al., 2016). Our *in-silico* analysis of putative Fae in *M. oryzae* showed the presence of conserved GXSXG motif and were found to belong to α/β-hydrolase-fold superfamily.

Often, CWDEs are found as an expanded gene family in phytopathogenic fungi and are difficult to specifically characterize mainly due to tight transcriptional regulation and functional redundancy of the members of the gene family i.e., loss of function of one gene is often compensated by the other genes in the family. Our HMM-based domain analysis across different fungal species showed a significant genetic diversity in the Fae sequences therein. Importantly, absence of any putative Fae in budding and fission yeasts suggests that the enzyme from other, especially phytopathogenic, fungal species could be associated mainly with degradation of plant cell walls. Similarly, presence of large number of Fae sequences in non-pathogenic filamentous fungi such as *Aspergillus spp*. and *N. crassa* is intriguing and studies on *FAE*s across different fungal genera could possibly shed some light on any evolutionary aspect of it. Indeed, our phylogenetic analysis revealed that the *M. oryzae* Fae1 (MGG_08737) has evolutionarily diverged more as compared to its paralogs and orthologs across different fungi. In *M. oryzae*, previous studies were aimed at understanding the role of endo-xylanases (Nguyen et al., 2011) and cellulases (Vu et al., 2012) in fungal pathogenesis,

by simultaneous silencing of multiple genes. Similarly, Cutinase2 (one out of the three putative Cutinases), which was significantly induced during host penetration stage, plays a role in full virulence in *M. oryzae* (Skamnioti and Gurr, 2007). In the present study, we investigated the role of one of the feruloyl esterases (Fae1) in pathogenicity of *M. oryzae*.

We found that the extracellular feruloyl esterase activity in the blast fungus was significantly increased in the presence of rice leaf extract. Possibly, *FAE*s were induced by the complex mixture of host factor(s) including the individual plant cell wall components. Thus, we studied the expression pattern of all the *FAE* genes under host- or pathogenicity-mimic conditions. We found that *FAE* genes expressed differentially, with majority of them accumulating >1.5 fold higher, in response to individual plant cell wall components. While our observation is consistent with a previously reported similar upregulation of *FAE*s in *Aspergillus niger* (de Vries et al., 2002) and *Fusarium graminearum* (Balcerzak et al., 2012), it remains to be tested whether a combination of more than one host cell wall component would cause further upregulation in *FAE* expression Intriguingly, majority of the *FAE*s were significantly upregulated in the presence of N-acetylglucosamine (NAG). A secreted *M. oryzae* chitinase (MoChia1), that binds to chitin to suppress plant immune response during infection (Yang et al., 2019), could likely digest free chitin to monomeric NAG, which in turn could be sensed by the blast fungus to express Fae. However, this hypothesis needs to be tested further.

A recent study on transcriptome profiling showed that MGG_08737 significantly upregulates at 18 hpi (161-fold), 27 hpi (82-fold), 36 hpi (130-fold), 45 hpi (147-fold) and 72 hpi (228-fold) during infection cycle of *M. oryzae* (Jeon et al., 2020). We found a similar pattern, where *FAE1* was specifically upregulated during both pre-invasive appressorial development

(12 and 24 hpi) and post-penetration host colonisation stages (48 to 72 hpi) of the infection cycle. Accordingly, loss of Fae1 function specifically impaired the ability of *M. oryzae* to invade and colonize rice, barley and wheat tissue. Although our *in silico* analysis suggested that the Fae function could be attributed to specific hosts, the defect in the *fae1*Δ mutant could not be correlated to any of the host species used in this study. However, it remains to be studied whether *fae1*Δ has a distinct phenotype with any other cereal crops. Further, very few appressoria (<5%) that were able to form invasive hyphae in the mutant were defective in spreading to the adjacent host cells and were rather restricted to the first cell invaded, even after prolonged incubation (96 hpi). Our observations are in line with the hypothesis that Fae, and CWDEs in general, likely play an important role in cell-to-cell spread of the fungus within the host tissue, and subsequent necrotrophic growth phase (Zheng et al., 2009). We were intrigued by our observation that the deletion of just one *FAE* led to a significant defect in host invasion and that the presence of none other putative *FAE* could compensate for the loss of Fae1 function. Interestingly, our *in silico* analysis suggests that Fae1, among all the *M. oryzae FAE*s, is highly diverged (Fig. 1B) and that there is no significant identity between any two Fae proteins in *M. oryzae* (Supplementary Fig. S5). This might possibly explain why the loss-of-function of Fae1 alone led to a significant phenotype in *M. oryzae*.

During appressorial development, the blast fungus derives energy by utilizing stored lipids via β-oxidation in the mitochondria and peroxisomes, generating acetyl-CoA, which is further distributed into the glyoxylate cycle and gluconeogenesis (Wang et al., 2007; Patkar et al., 2012). It is hypothesized that this metabolic process might be required to support the initial appressorial development and maturation, which ensures host penetration by the blast fungus, and the subsequent energy requirement during host tissue colonisation could be fulfilled by the host-derived nutrients (Fernandez and Wilson, 2014). It is possible that the plant cell wall

carbohydrates released after CWDEs activity could act as an energy source for the fungus at the host-pathogen interface and facilitate its entry and/or elaboration into the host. Feruloyl esterases in *Aspergillus niger* act synergistically, with other CWDEs like cellulases, xylanases and pectinases, to degrade the complex plant cell wall carbohydrates (Faulds and Williamson, 1995). In *M. oryzae*, endo-xylanases (Nguyen et al., 2011) and cellulases (Vu et al., 2012) are shown to be important in host-penetration and virulence of the blast fungus. Considering all this, we wondered whether sugar released from CWDE-mediated plant cell wall digestion could act as an energy source for the fungus. Indeed, exogenous supply of glucose rescued the *fae1*Δ strain, indicating that the mutant was deprived of energy source at the time of host invasion. Interestingly, exogenous supply of ferulic acid, which is a product of Fae enzyme action, could also moderately support the invasive growth of the *fae1*Δ mutant. This is in accordance with a previous hypothesis that ferulic acid could possibly act as a weak or an alternative carbon source (Black and Dix, 1976; Fig. 6C). Here, we propose that, like in *A. niger*, the Fae in *M. oryzae* acts, in a concerted manner, on the esterified ferulic acid bridges in the plant cell wall to allow endo-xylanases and cellulases to work on the carbohydrates therein, releasing constituent sugar molecules and ferulic acid, which could act as the energy source during host invasion (Fig. 7).

Feruloyl esterases have a wide range of applications in biofuel industry, food, cosmetic and pharmaceutical industry and also paper and pulp industry, all of which involve plant biomass degradation (Dilokpimol et al., 2016). It is often used in conjunction with other plant cell wall deconstructing enzymes. Most of the applied aspects of feruloyl esterases have been studied in *Aspergillus spp*. Although *M. oryzae* is a phytopathogenic fungus, one could explore the potential use of recombinantly expressed Fae1 in industrial applications, both in terms of enzyme activity and range of substrate specificity. Similarly, ferulic acid, the

552 product of feruloyl esterase enzyme action, has a large application in food and
553 pharmaceutical industry (Dilokpimol et al., 2016). Thus, use of an efficient feruloyl esterase
554 (*M. oryzae* Fae1) for production of ferulic acid could also be explored. Moreover, it has been
555 reported that Fae can also act on synthetic esterified substrates such as methyl ferulate,
556 methyl sinapate, methyl *p*-coumarate and methyl caffeate (Crepin et al., 2004). Therefore, it
557 would be worth exploring whether or not Fae1, or feruloyl esterases in general, can also act
558 on rutin complexed with glucose, thereby releasing quercetin, a plant flavanol with medicinal
559 properties. This might also implicate another potential commercial application of Fae.
560 Further, given the involvement of Fae1 specifically in pathogenicity of *M. oryzae*, it could be
561 considered as a potential target for developing an antifungal strategy.
562
563 Altogether, we show that the *M. oryzae* feruloyl esterase Fae1 plays a key role in
564 pathogenesis, wherein the enzyme activity likely makes the alternative energy source
565 available and supports the fungal growth during host invasion and colonisation.

566

567

568 **Acknowledgements**

569 We acknowledge late Prof. Bharat B. Chattoo for his guidance and providing sophisticated
570 laboratory facility at the Bharat Chattoo Genome Research Centre (BCGRC). We also fondly
571 remember late Dr. Johannes Manjrekar for the useful scientific discussions during the course
572 of this work. We thank Naweed Naqvi (Temasek Lifesciences Laboratory, Singapore) for
573 providing backbone vector pFGL1010. AT was supported by UGC-BSR-RFSMS (F.7-
574 128/2007-BSR, dtd-02.09.2014), University Grants Commission, Government of India; and
575 KM acknowledges the intramural University Research Scholarship from The M. S.

University of Baroda. This work was supported by the Ramalingaswami Fellowship, DBT, GoI (BT/RLF/Re-entry/32/2014) awarded to RP. We thank the BCGRC group at MSU for useful discussions.

Author contributions

Conceptualization: AT and RP; Methodology: AT and RP; Validation: AT and KM; Formal analysis: AT; Investigation: AT and KM; Resources: RP; Writing - original draft: AT and KM; Writing - review and editing: RP; Supervision: RP; Project administration: RP; Funding acquisition: RP.

Declarations:

Competing interests - Authors declare that there are no competing interests involved in this work.

Ethics approval - Not applicable.

Consent to participate - Not applicable.

Consent for publication - Not applicable.

Reference:

1. Balcerzak, M., Harris, L. J., Subramaniam, R., Ouellet, T., 2012. The feruloyl esterase gene family of *Fusarium graminearum* is differentially regulated by aromatic compounds and hosts. *Fungal Biol.* **116:** 478–488.

2. Biswas, S., Dijck, P.V., Datta, A., 2007. Environmental sensing and signal transduction pathways regulating morphopathogenic Determinants of *Candida albicans*. *Microbiol. Mol. Biol. Rev.* **71:** 348–376.

3. Black, R. L. B., Dix, N. J., 1976. Utilization of ferulic acid by microfungi from litter and soil. *Transact. British Mycol. Soc.* **66:** 313–317.

4. Bunzel, M., Ralph, J., Marita, J. M., Hatfield, R. D., Steinhart, H., 2001. Diferulates as structural components in soluble and insoluble cereal dietary fibre. *J. Sci. Fd. Agric.* **81:** 653–660.

5. Capella-Gutiérrez, S., Silla-Martínez, J. M., Gabaldón, T., 2009. trimAl: A tool for automated alignment trimming in large-scale phylogenetic analyses. *Bioinformatics* **25:** 1972–1973.

6. Cosgrove, D. J., 2001. Wall structure and wall loosening. A look backwards and forwards. *Plant Physiol.* **125:** 131–134.

7. Crepin, V. F., Faulds, C. B., Connerton, I. F., 2004. Functional recognition of new classes of feruloyl esterases. *Appl. Microbiol. Biotechnol.* **63:** 647–652.

8. De Vries, R. P., Michelsen, B., Poulsen, C. H., Kroon, P. A., van den Heuvel, R. H. H., et al., 1997. The faeA genes from *Aspergillus niger* and *Aspergillus tubingensis* encode ferulic acid esterases involved in degradation of complex cell wall polysaccharides. *Appl. Environ. Microbiol.* **63:** 4638–4644.

9. De Vries, R. P., Vankuyk, P. A., Kester, H. C. M., Visser, J., 2002. The *Aspergillus niger faeB* gene encodes a second feruloyl esterase involved in pectin and xylan degradation and is specifically induced in the presence of aromatic compounds. *Biochem. J.* **363:** 377–386.

10. Dean, R. A., Talbot, N. J., Farman, M. L., Mitchell, T. K., Orbach, M. J., et al., 2005. The genome sequence of the rice blast fungus *Magnaporthe grisea*. *Nature* **434:** 980–986.

11. Dellaporta, S. L., Wood, J., Hicks, J. B., 1983. A plant DNA minipreparation: Version II. *Plant Mol. Biol. Rep.* **1:** 19–21.

12. Dilokpimol, A., Makela, M. R., Anguilar-Pontes, M. V., Benoit-Gelber, I., Hidden, K. S., et al., 2016. Diversity of fungal feruloyl esterases: updated phylogenetic classification, properties, and industrial applications. *Biotechnol. Biofuels* **9:** 231.

13. Ebbole, D. J., 2007. *Magnaporthe* as a model for understanding host-pathogen interactions. *Annu. Rev. Phytopathol.* **45:** 437–456.

14. Faulds, C. B., Williamson, G., 1994. Purification and characterization of a ferulic acid esterase (FAEIII) from *Aspergillus niger*: specificity for the phenolic moiety and binding to micro-crystalline cellulose. *Microbiology* **140:** 779–787.

15. Faulds, C. B., Williamson, G., 1995. Release of ferulic acid from wheat bran by a ferulic acid esterase (FAE-III) from *Aspergillus niger*. *Appl. Microbiol. Biotechnol.* **43:** 1082–1087.

16. Fernandez, J., Wilson, R. A., 2014. Cells in cells: morphogenetic and metabolic strategies conditioning rice infection by the blast fungus *Magnaporthe oryzae*. *Protoplasma* **251:** 37–47.

17. Gietz, R. D., Woods, R. A., 2002. Transformation of yeast by lithium acetate/single-stranded carrier DNA/polyethylene glycol method. *Methods Enzymol*. **350**: 87–96.

18. Hancock, J. M., Bishop, M. J., 2004. HMMer. In *Dictionary of Bioinformatics and Computational Biology* (Vol. 1–June). John Wiley & Sons, Ltd.

19. Harris, P. J., Hartley, R. D., 1977. Detection of bound ferulic acid in cell walls of the Gramineae by ultraviolet fluorescence microscopy. *Nature* **259:** 508–510.

20. Hermoso, J. A., Aparicio, J. S., Molina, R., Juge, N., Gonzalez, R., et al., 2004. The crystal structure of Feruloyl esterase A from *Aspergillus niger* suggests evolutive functional convergence in feruloyl esterase family. *J. Mol. Biol.* **338:** 495–506.

21. Howard, R. J., Ferrari, M. A., Roach, D. H., Money, N. P., 1991. Penetration of hard substrates by a fungus employing enormous turgor pressure. *Proc. Natl. Acad. Sci. U.S.A.* **88:** 11281–11284.

22. Jeon, J., Lee, G. W., Kim, K. T., Park, S. Y., Kim, S., et al., 2020. Transcriptome profiling of the rice blast fungus *Magnaporthe oryzae* and its host *Oryza sativa* during infection. *Mol. Plant Microbe Interact*. **33:** 141–144.

23. Kachroo, P., Lee, K. H., Schwerdel, C., Bailey, J. E., Chattoo, B. B., 1997. Analysis of host-induced response in the rice blast fungus *Magnaporthe grisea* using two-dimensional polyacrylamide gel electrophoresis. *Electrophoresis*. **18:** 163–169.

24. Kachroo, P., Leong, S. A., Chattoo, B. B., 1994. Pot2, an inverted repeat transposon from the rice blast fungus *Magnaporthe grisea*. *Mol. Gen. Genet.* **245:** 339–348.

25. Kubicek, C. P., Starr, T. L., Glass, N. L., 2014. Plant cell wall-degrading enzymes and their secretion in plant-pathogenic fungi. *Annu. Rev. Phytopathol.* **52:** 427–451.

26. Kumar, S., Stecher, G., Tamura, K., 2016. MEGA7: Molecular Evolutionary Genetics Analysis Version 7.0 for Bigger Datasets. *Mol. Biol. Evol.* **33:** 1870–1874.

27. Lee, S., Kelley, B. S., Damasceno, C. M. B., St. John, B., Kim, B., et al., 2006. A functional screen to characterize the secretomes of eukaryotic pathogens and their hosts *in planta*. *Mol. Plant Microbe Interact.* **19:** 1368–1377.

28. Letunic, I., Bork, P., 2019. Interactive Tree Of Life (iTOL) v4: Recent updates and new developments. *Nucleic Acids Res.* **47(W1):** W256–W259.

29. Livak, K. J., Schmittgen, T. D., 2001. Analysis of relative gene expression data using real-time quantitative PCR and the $2^{-\Delta\Delta CT}$ method. *Methods* **25:** 402–408.

30. Marchler-Bauer, A., Derbyshire, M. K., Gonzales, N. R., Lu, S., Chitsaz, F., et al., 2015. CDD: NCBI's conserved domain database. *Nucleic Acids Res*. **43**(Database issue): D222–D226.

31. Mastihuba, V., Kremnicky, L., Mastihubova, M., Willett, J. L., Cote, G. L., 2002. A spectrophotometric assay for feruloyl esterases. *Anal. Biochem.* **309:** 96–101.

675 32. Nguyen, L.-T., Schmidt, H. A., von Haeseler, A., Minh, B. Q., 2015. IQ-TREE: A
676 Fast and Effective Stochastic Algorithm for Estimating Maximum-Likelihood
677 Phylogenies. *Mol. Biol. Evol.* **32:** 268–274.

678 33. Nguyen, Q. B., Itoh, K., Vu, V. B., Tosa, Y., Nakayashiki, H., 2011. Simultaneous
679 silencing of endo-β-1,4 xylanase genes reveals their roles in the virulence of
680 *Magnaporthe oryzae*. *Mol. Microbiol.* **81:** 1008–1019.

681 34. Patkar, R. N., Benke, P. I., Qu, Z., Chen, Y., Yang, F., et al., 2015. A fungal
682 monooxygenase-derived jasmonate attenuates host innate immunity. *Nat. Chem.*
683 *Biol.* **11:** 733–740.

684 35. Patkar, R. N., Ramos-Pamplona, M., Gupta, A. P., Fan, Y., Naqvi, N. I., 2012.
685 Mitochondrial β-oxidation regulates organellar integrity and is necessary for conidial
686 germination and invasive growth in *Magnaporthe oryzae*. *Mol. Microbiol*. **86:** 1345–
687 1363.

688 36. Patkar, R. N., Suresh, A., Naqvi, N. I., 2010. MoTea4-mediated polarized growth is
689 essential for proper asexual development and pathogenesis in *Magnaporthe oryzae*.
690 *Eukaryot. Cell* **9:** 1029–1038.

691 37. Petersen, T. N., Brunak, S., Heijne, G., Nielsen, H., 2011. SignalP 4.0: discriminating
692 signal peptides from transmembrane regions. *Nat. Methods* **8:** 785–786.

693 38. Prakash, C., Manjrekar, J., Chattoo, B. B., 2016. Skp1, a component of E3 ubiquitin
694 ligase, is necessary for growth, sporulation, development and pathogenicity in rice
695 blast fungus (*Magnaporthe oryzae*). *Mol. Plant Pathol*. **17:** 903–919.

696 39. Sievers, F., Higgins, D. G., 2018. Clustal Omega for making accurate alignments of
697 many protein sequences. *Protein Sci.* **27:** 135–145.

698 40. Sievers, F., Wilm, A., Dineen, D., Gibson, T.J., Karplus, K., et al., 2011. Fast,
699 scalable generation of high-quality protein multiple sequence alignments using
700 Clustal Omega. *Mol. Syst. Biol.* **7:** 539.

701 41. Skamnioti, P., Gurr, S. J., 2007. *Magnaporthe grisea* Cutinase2 mediates
702 appressorium differentiation and host penetration and is required for full virulence.
703 *Plant Cell* **19:** 2674–2689.

704 42. Skamnioti, P., Gurr, S. J., 2008. Against the grain: safeguarding rice from rice blast
705 disease. *Trends Biotechnol.* **27:** 141–150.

706 43. Soundararajan, S., Jedd, G., Li, X., Ramos-Pamploña, M., Chua, N. H., et al., 2004.
707 Woronin body function in *Magnaporthe grisea* is essential for efficient pathogenesis
708 and for survival during nitrogen starvation stress. *The Plant cell* **16:** 1564–1574.

709 44. Valent, B., Khang, C. H., 2010. Recent advances in rice blast effector research. *Curr*
710 *Opin Plant Biol*. **13:** 434–441.

711 45. Vu, B. V., Itoh, K., Nguyen, Q. B., Tosa, Y., Nakayashiki, H., 2012. Cellulases
712 belonging to glycoside hydrolase families 6 and 7 contribute to the virulence of
713 *Magnaporthe oryzae*. *Mol. Plant Microbe Interact*. **25:** 1135–1141.

714 46. Wang, Z. Y., Soanes, D. M., Kershaw, M. J., Talbot, N. J., 2007. Functional analysis
715 of lipid metabolism in *Magnaporthe grisea* reveals a requirement for peroxisomal
716 fatty acid beta-oxidation during appressorium-mediated plant infection. *Mol. Plant*
717 *Microbe Interact*. **20:** 475–491.

718 47. Xu, M., Gao, X., Chen, J., Yin, Z., Feng, H., Huang, L., 2017. The feruloyl esterase
719 genes are required for full pathogenicity of the apple tree canker pathogen *Valsa mali*.
720 *Mol. Plant Pathol*. **19:** 1353–1363.

721 48. Yang, C., Yu, Y., Huang, J., Meng, F., Pang, J., et al., 2019. Binding of the
722 *Magnaporthe oryzae* chitinase MoChia1 by a rice tetratricopeptide repeat protein
723 allows free chitin to trigger immune responses. *Plant Cell* **31:** 172–188.

724 49. Yang, F., Naqvi, N., 2014. Sulfonylurea resistance reconstitution as a novel strategy
725 for *ILV2*-specific integration in *Magnaporthe oryzae*. *Fungal Genet Biol.* **68**: 71–6.

726 50. Yu, J. H., Hamari, Z., Han, K. H., Seo, J. A., Reyes-Domínguez Y, et al., 2004.
727 Double-joint PCR: a PCR-based molecular tool for gene manipulations in filamentous
728 fungi. *Fungal Genet. Biol*. **41:** 973–981.

729 51. Zheng, X., Zhou, J., Lin, C., Lin, X., Lan, L., et al., 2009. Secretion property and gene
730 expression pattern of a putative feruloyl esterase in *Magnaporthe grisea*. In: Xiaofan,
731 W., Valent, B. (eds), *Advances in genetics, genomics and control of rice blast disease*,
732 1st edn. Springer, Netherlands, pp. 41–50.

Figure legends:

Figure 1. Identification and phylogenetic analysis of putative fungal Fae. **(A)** Multiple sequence alignment of putative Fae sequences from *M. oryzae*, *A. oryzae* and *N. crassa*. The conserved GXSXG motif is marked with a red box. **(B)** Phylogenetic analysis of Fae sequences from 21 fungal species representing seven classes. The phylogenetic tree is based on maximum likelihood methods, with assessment of branch support by 1000 replicates of ultrafast bootstrap. Tree branches are color-coded according to the specific fungal species. The colors in the outer and inner circular strips represent taxonomy, for each branch, with respect to fungal class and species, respectively. Bootstrap values are indicated as grey circles, sized according to the values. Grey highlighted background represents the sub-clades belonging to the *Magnaporthales* order. Stars denote Fae proteins from *M. oryzae*; filled-star marks the MGG_08737 gene used in the present study. Stars in clockwise direction - putative Fae encoded by MGG_09677, MGG_09732, MGG_03502, MGG_02261, MGG_05592, MGG_05366, MGG_09404, MGG_03771, and MGG_08737, respectively. **(C)** Phylogenetic tree depicting combined analysis of Fae sequences in host-specific *M. oryzae* isolates from rice (*Oryza*; pink), wheat (*Triticum*; blue), foxtail millet (*Setaria*; purple) and finger millet (*Eleusine*; green).

Figure 2. *M. oryzae* feruloyl esterases are secretory in nature and induced by host leaf extract. (A) A schematic representation of the Yeast Secretion Trap strategy used to study presence of a signal peptide in Fae. **(B)** The Yeast Secretion Trap based assay depicting growth of the transformants expressing *M. oryzae FAE* (MGG_05529 or MGG_07294) when compared to the no-growth, on SD + Sucrose, of the recipient strain (DBYα2445) with or without the backbone vector (pYST). **(C)** A bar chart showing Fae enzyme activity in the

intracellular versus extracellular (secretory) fraction of the *M. oryzae* culture grown in the presence or absence of rice leaf extract. The data is represented as mean ± s.d.m. from three independent experiments. ***, $P < 0.001$.

Figure 3. Differential expression of feruloyl esterase genes during pathogenesis in *M. oryzae*. (A) A bar chart showing relative transcript levels of nine *FAE*s in *M. oryzae* vegetative culture grown under different conditions. The cultures were grown in minimal medium with either 0.03% cutin monomers (1, 16 - hexadecanediol), 0.03% ferulic acid, nitrogen-starvation, 1% Pectin, 1% N-acetylglucosamine (NAG) or 1% Xylan, for 48 h before harvesting the biomass. The *FAE* transcript levels were estimated relative to those in the vegetative culture grown in minimal medium containing 1% glucose as a control condition. The horizontal line corresponding to the fold change 1 represents normalized transcript levels for the control condition. **(B)** A bar chart depicting relative transcript levels of nine *FAE*s during different stages of pathogenic development. Samples were harvested at the time points mentioned and the transcript levels were compared to those from vegetative mycelia as control condition. β-tubulin was used as an endogenous control in both (A) and (B). Data represents mean values ± s.d.m. from three independent biological replicates with technical triplicates each time.

Figure 4. Fae1 function is not required for vegetative and host-independent early pathogenic development in *M. oryzae*. Vegetative growth of the WT or *fae1*Δ on prune agar plates at 10 dpi **(A)** with measurements of diameter of colonies of both the strains shown in **(B)**. Data represents mean ± s.d.m. from the experiments repeated thrice. **(C)** A bar graph depicting total conidiation assessed by counting the number of conidia harvested at 10 dpi

781 from the WT or *fae1*Δ culture grown on PA plates. Data represents mean ± s.d.m. from three
782 independent experiments. ns, not significant. **(D)** Micrographs showing appressorial
783 development, on an inductive glass surface, in the WT or *fae1*Δ, at 24 hpi. Scale bar, 10 μm.
784 **(E)** A quantitative analysis of appressorial development in the WT or *fae1*Δ at 24 hpi. Data
785 represents mean ± s.d.m. from three independent experiments, with at least 100 appressoria
786 each observed for quantification. ns, not significant.

787

788 **Figure 5. Fae1 function is crucial for host invasion and colonisation during blast**
789 **disease. (A)** Whole-plant infection assay depicting blast disease outcome from the rice plants
790 spray-inoculated with either the WT, *fae1*Δ or *fae1*Δ/*FAE1* conidia or *fae1*Δ supplemented at
791 22 hpi with 2% glucose or 100 mM ferulic acid. The representative leaves were detached and
792 photographed after 6 dpi. **(B)** Micrographs showing host invasion (~48 hpi) ability of either
793 the WT, *fae1*Δ mutant, *fae1*Δ/*FAE1* or *fae1*Δ supplemented with 2% glucose or 100 mM
794 ferulic acid. Glucose or ferulic acid was added after 22 hpi. Images were taken at ~48 hpi.
795 Asterisks mark appressoria, while arrowheads depict the invasive hyphae. Yellow asterisks
796 mark the non-invading *fae1*Δ appressoria and the arrow depicts the invasive hypha restricted
797 to the first invaded host (rice sheath) cell. Scale bar, 10 μm. **(C)** A bar chart depicting
798 percentage of appressoria invading the rice sheath inoculated with either the WT, *fae1*Δ,
799 *fae1*Δ/*FAE1* or *fae1*Δ supplemented with 2% glucose or 100 mM ferulic acid. Data
800 represents mean ± s.d.m. from three independent experiments, with at least 100 appressoria
801 each observed for quantification. ***, $P < 0.001$; ns, not significant.

802

803 **Figure 6. Ferulic acid released by the Fae1 action is likely required as a nutrient source**
804 **during host invasion and colonisation by *M. oryzae*. (A)** Drop-inoculation assay showing

infection ability (on detached rice leaves) of WT, *fae1*Δ or *fae1*Δ supplemented with 100 mM ferulic acid (FA) or 20 mM reduced glutathione (GSH). Images were taken at 6 dpi. **(B)** Leaf sheath inoculation assay showing host invasion ability of the WT or *fae1*Δ supplemented with 20 mM GSH, which was added at 22 hpi. The results were observed at 48 hpi. White and yellow asterisks mark the invading and non-invading appressoria, respectively. Arrow depicts invasive hypha restricted to the first host cell invaded. Scale bar, 10 μm. **(C)** Vegetative growth of the WT *M. oryzae* on basal medium (BM) with or without 0.01% ferulic acid. The images were taken at 10 dpi.

Figure 7. A proposed model of Fae1 function during pathogenesis in *M. oryzae*. Fae1, likely secreted along with other CWDEs, hydrolyses the plant cell wall to release ferulic acid and constituent carbohydrates during penetration of the first host cell and subsequent spread to the neighbouring cells. Released ferulic acid, the product of Fae enzyme action, and/or glucose, the breakdown product of cellulose, likely act as an energy source enabling successful host-invasion and colonisation by the blast fungal pathogen.

Figures

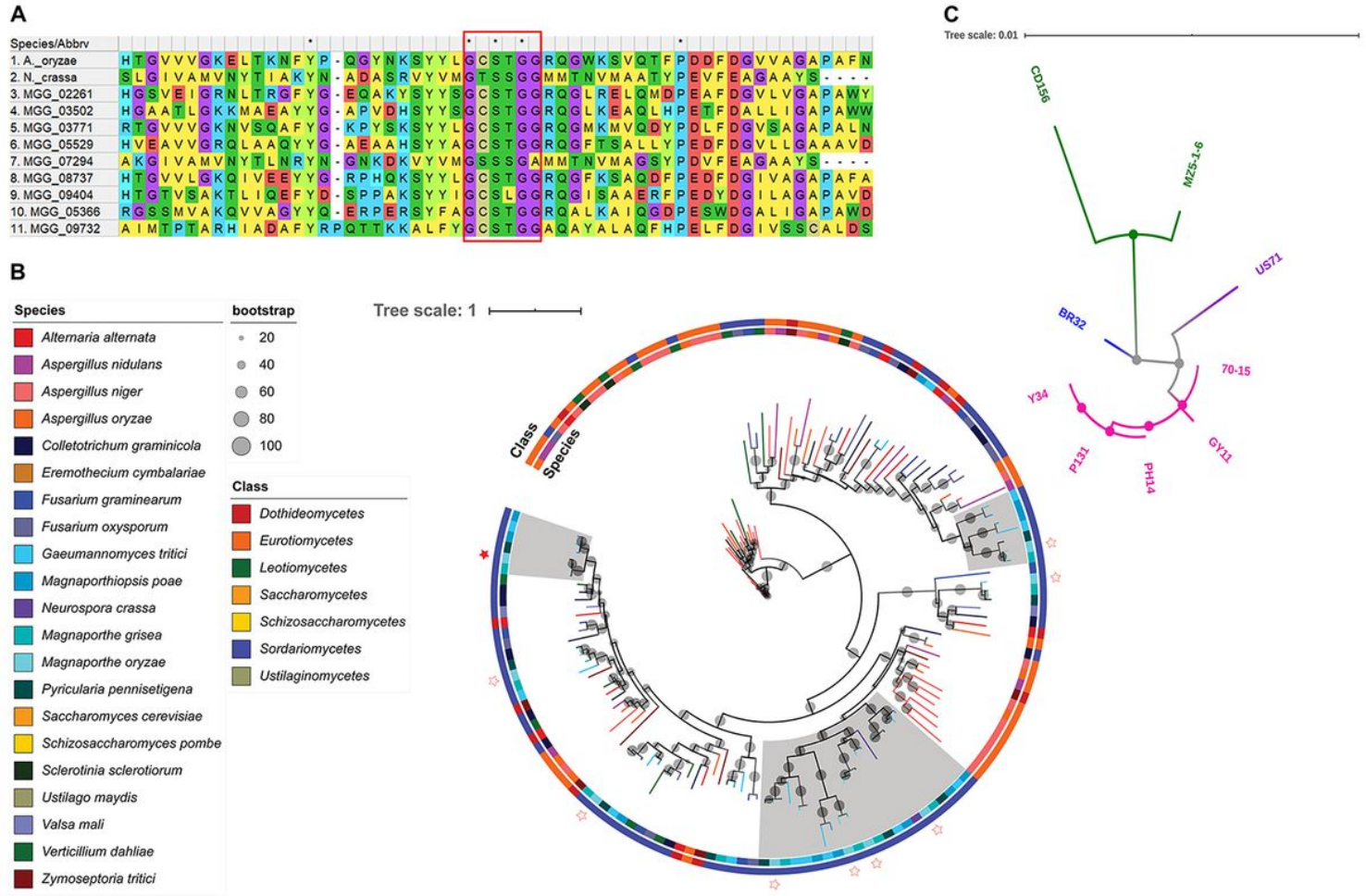

Figure 1

Identification and phylogenetic analysis of putative fungal Fae. (A) Multiple sequence alignment of putative Fae sequences from M. oryzae, A. oryzae and N. crassa. The conserved GXSXG motif is marked with a red box. (B) Phylogenetic analysis of Fae sequences from 21 fungal species representing seven classes. The phylogenetic tree is based on maximum likelihood methods, with assessment of branch support by 1000 replicates of ultrafast bootstrap. Tree branches are color-coded according to the specific fungal species. The colors in the outer and inner circular strips represent taxonomy, for each branch, with respect to fungal class and species, respectively. Bootstrap values are indicated as grey circles, sized according to the values. Grey highlighted background represents the sub-clades belonging to the Magnaporthales order. Stars denote Fae proteins from M. oryzae; filled-star marks the MGG_08737 gene used in the present study. Stars in clockwise direction - putative Fae encoded by MGG_09677, MGG_09732, MGG_03502, MGG_02261, MGG_05592, MGG_05366, MGG_09404, MGG_03771, and MGG_08737, respectively. (C) Phylogenetic tree depicting combined analysis of Fae sequences in host-specific M. oryzae isolates from rice (Oryza; pink), wheat (Triticum; blue), foxtail millet (Setaria; purple) and finger millet (Eleusine; green).

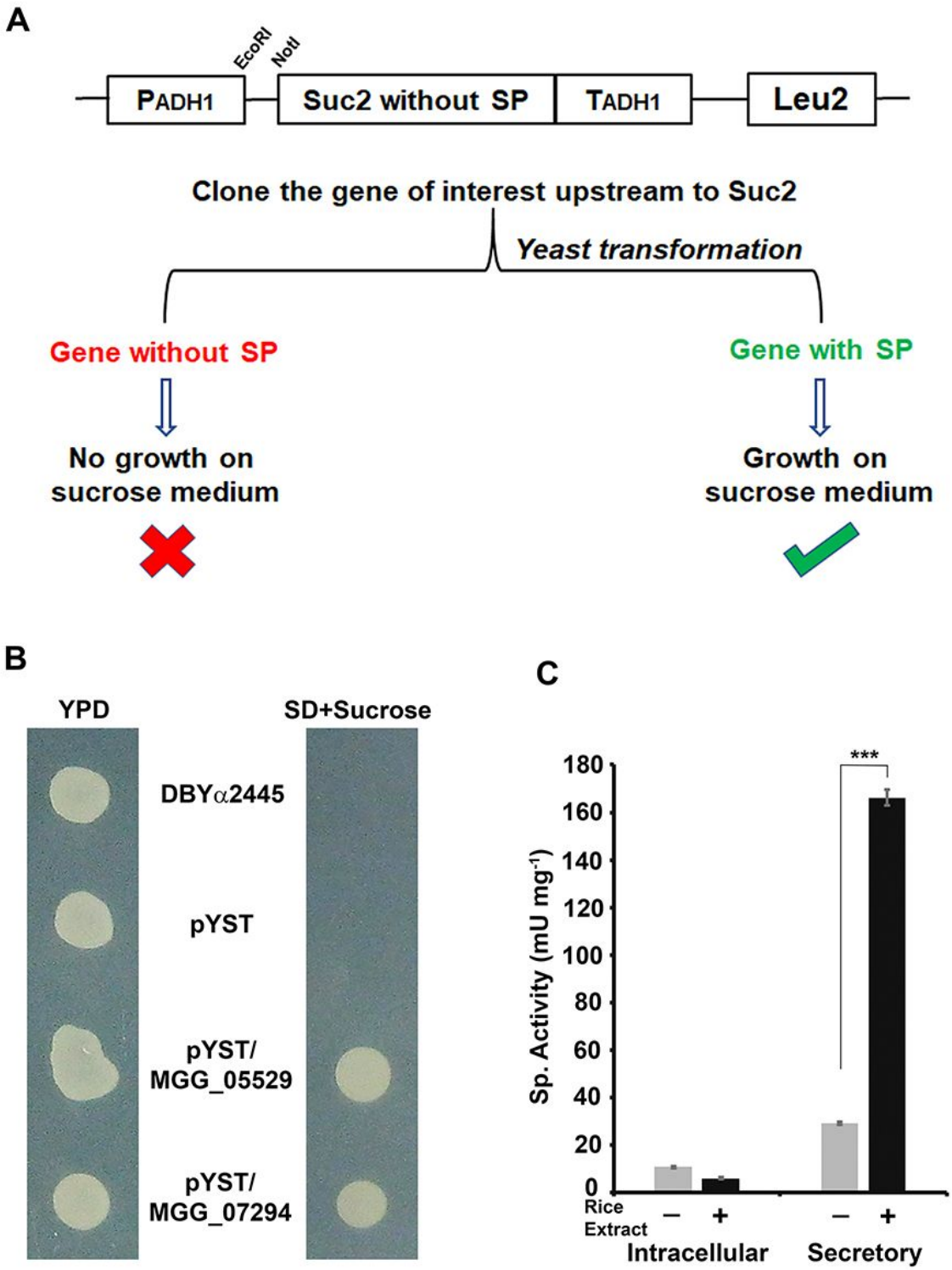

Figure 2

M. oryzae feruloyl esterases are secretory in nature and induced by host leaf extract. (A) A schematic representation of the Yeast Secretion Trap strategy used to study presence of a signal peptide in Fae. (B) The Yeast Secretion Trap based assay depicting growth of the transformants expressing M. oryzae FAE (MGG_05529 or MGG_07294) when compared to the no-growth, on SD + Sucrose, of the recipient strain (DBYα2445) with or without the backbone vector (pYST). (C) A bar chart showing Fae enzyme activity in

the intracellular versus extracellular (secretory) fraction of the M. oryzae culture grown in the presence or absence of rice leaf extract. The data is represented as mean ± s.d.m. from three independent experiments. ***, P < 0.001.

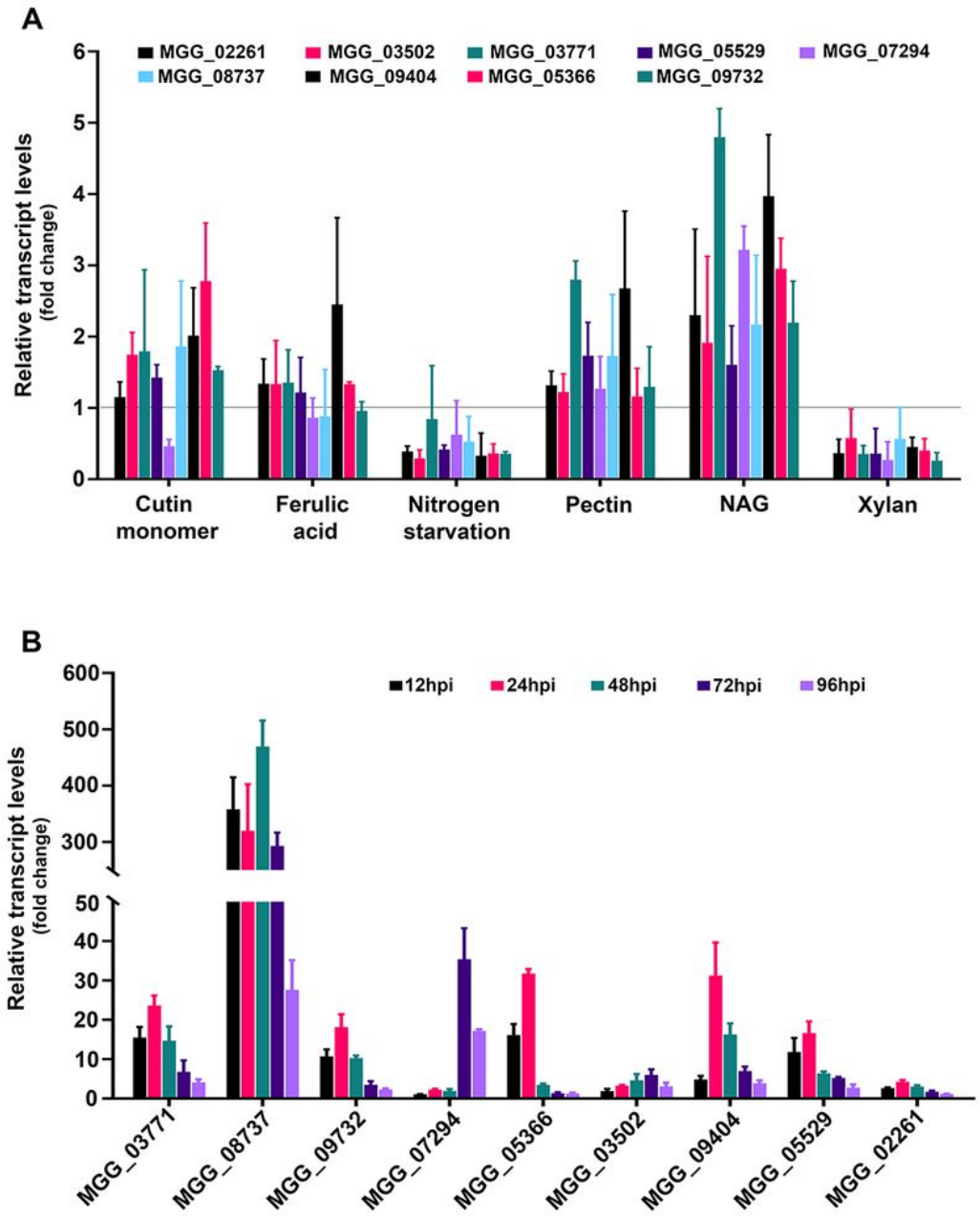

Figure 3

Differential expression of feruloyl esterase genes during pathogenesis in M. oryzae. (A) A bar chart showing relative transcript levels of nine FAEs in M. oryzae vegetative culture grown under different

conditions. The cultures were grown in minimal medium with either 0.03% cutin monomers (1, 16 - hexadecanediol), 0.03% ferulic acid, nitrogen-starvation, 1% Pectin, 1% N-acetylglucosamine (NAG) or 1% Xylan, for 48 h before harvesting the biomass. The FAE transcript levels were estimated relative to those in the vegetative culture grown in minimal medium containing 1% glucose as a control condition. The horizontal line corresponding to the fold change 1 represents normalized transcript levels for the control condition. (B) A bar chart depicting relative transcript levels of nine FAEs during different stages of pathogenic development. Samples were harvested at the time points mentioned and the transcript levels were compared to those from vegetative mycelia as control condition. β-tubulin was used as an endogenous control in both (A) and (B). Data represents mean values ± s.d.m. from three independent biological replicates with technical triplicates each time.

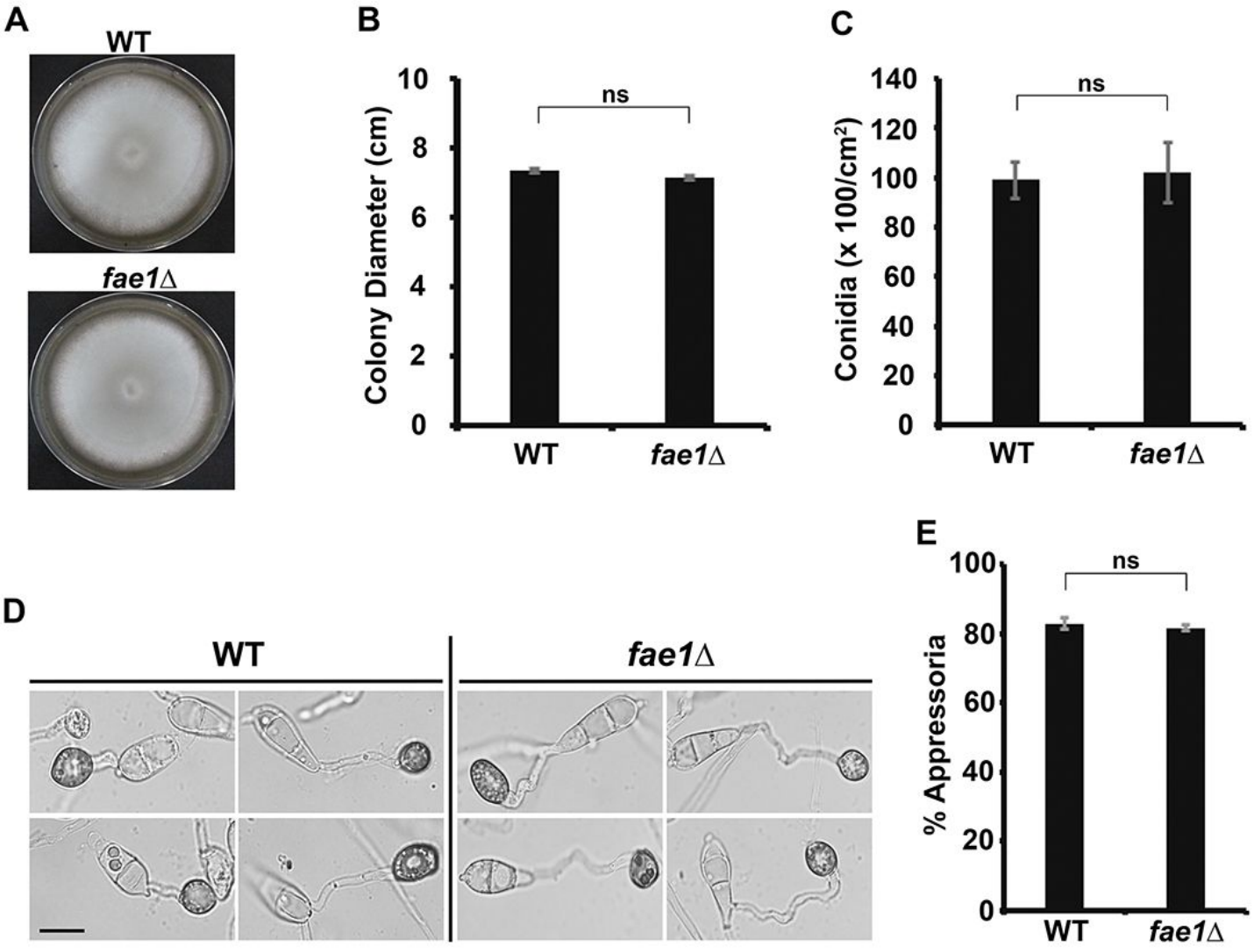

Figure 4

Fae1 function is not required for vegetative and host-independent early pathogenic development in M. oryzae. Vegetative growth of the WT or fae1Δ on prune agar plates at 10 dpi (A) with measurements of diameter of colonies of both the strains shown in (B). Data represents mean + s.d.m. from the

experiments repeated thrice. (C) A bar graph depicting total conidiation assessed by counting the number of conidia harvested at 10 dpi from the WT or fae1Δ culture grown on PA plates. Data represents mean + s.d.m. from three independent experiments. ns, not significant. (D) Micrographs showing appressorial development, on an inductive glass surface, in the WT or fae1Δ, at 24 hpi. Scale bar, 10 μm. (E) A quantitative analysis of appressorial development in the WT or fae1Δ at 24 hpi. Data represents mean ± s.d.m. from three independent experiments, with at least 100 appressoria each observed for quantification. ns, not significant.

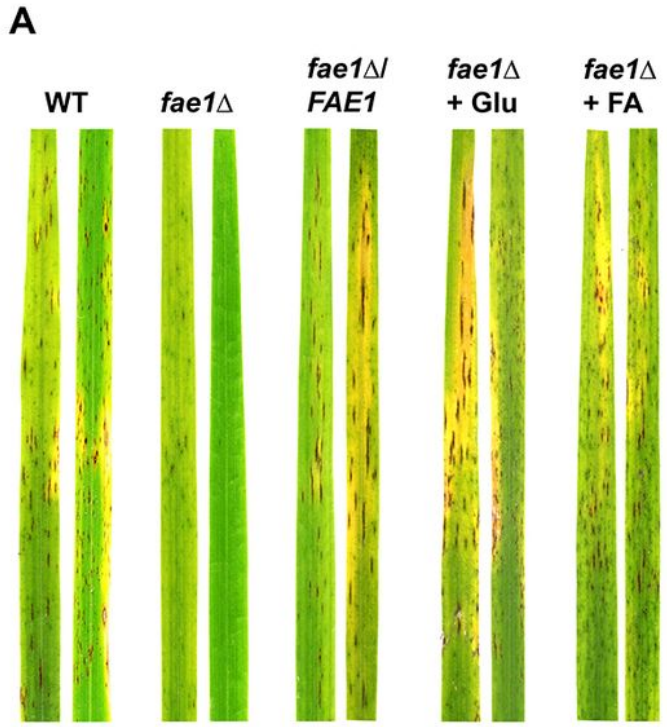

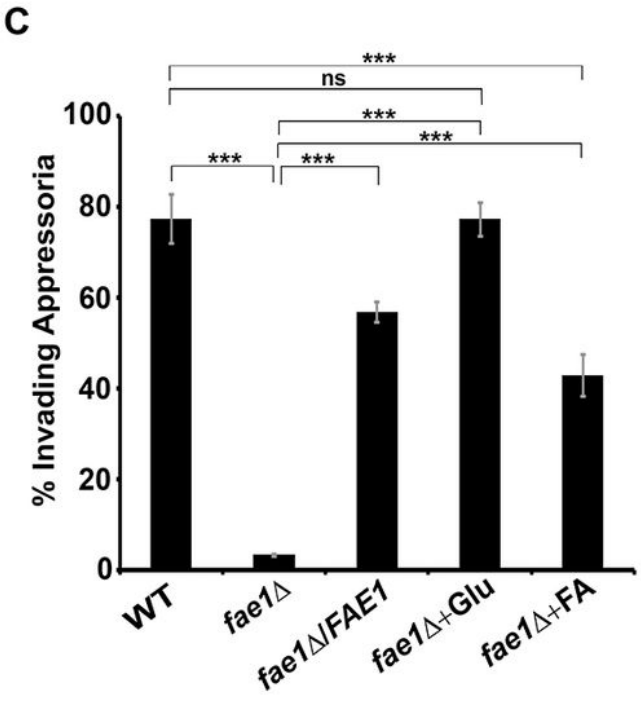

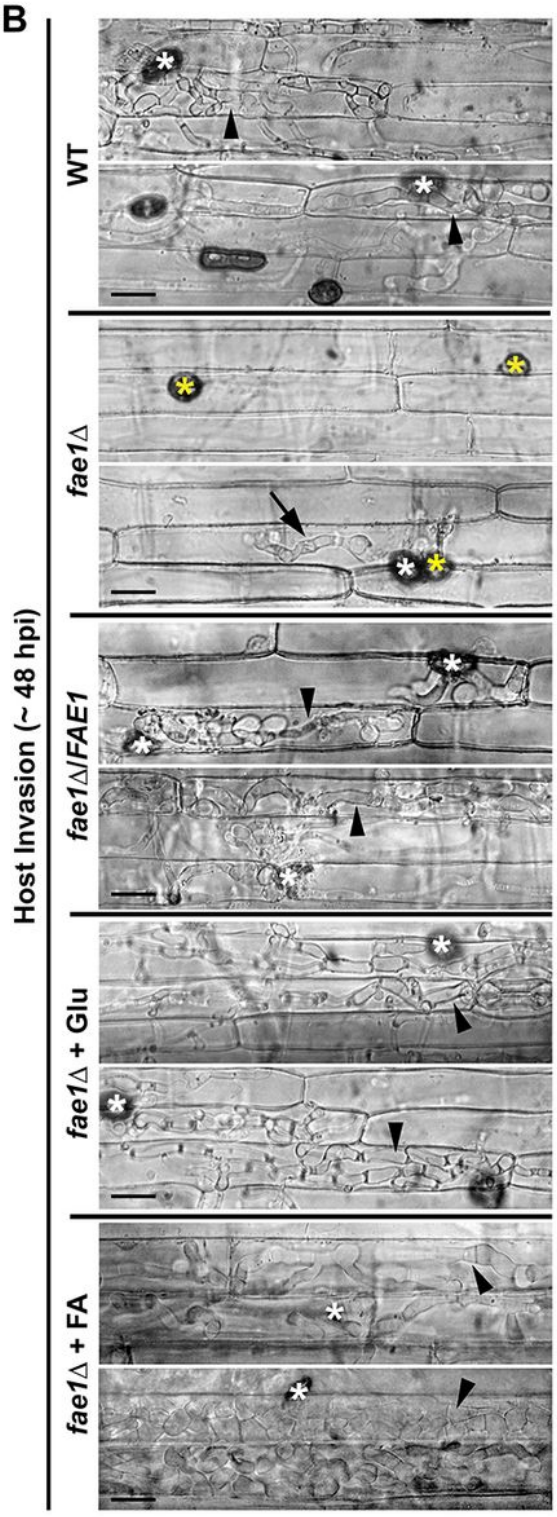

Figure 5

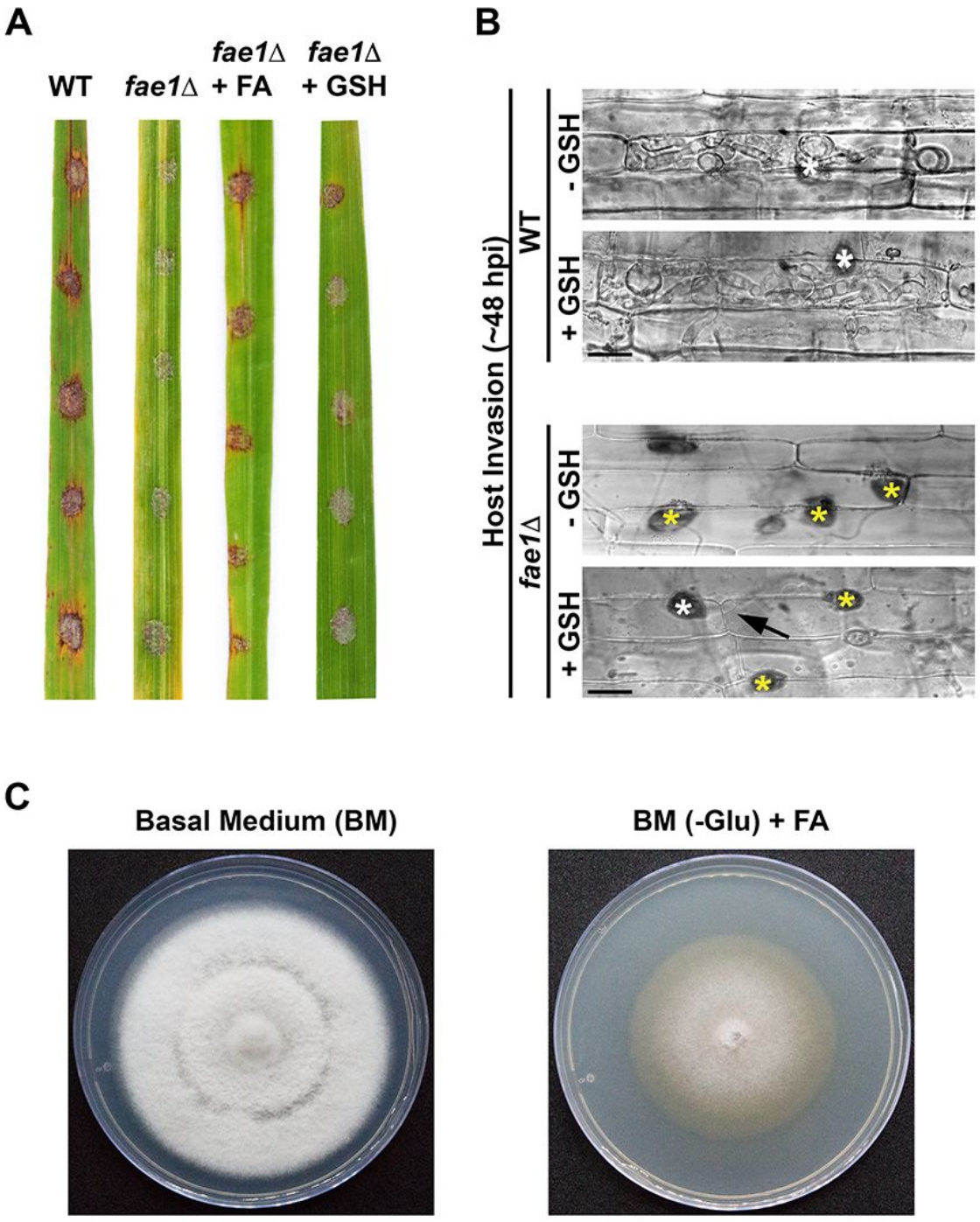

Figure 6

Ferulic acid released by the Fae1 action is likely required as a nutrient source during host invasion and colonisation by M. oryzae. (A) Drop-inoculation assay showing infection ability (on detached rice leaves) of WT, fae1Δ or fae1Δ supplemented with 100 mM ferulic acid (FA) or 20 mM reduced glutathione (GSH).

Images were taken at 6 dpi. (B) Leaf sheath inoculation assay showing host invasion ability of the WT or fae1Δ supplemented with 20 mM GSH, which was added at 22 hpi. The results were observed at 48 hpi. White and yellow asterisks mark the invading and non-invading appressoria, respectively. Arrow depicts invasive hypha restricted to the first host cell invaded. Scale bar, 10 µm. (C) Vegetative growth of the WT M. oryzae on basal medium (BM) with or without 0.01% ferulic acid. The images were taken at 10 dpi.

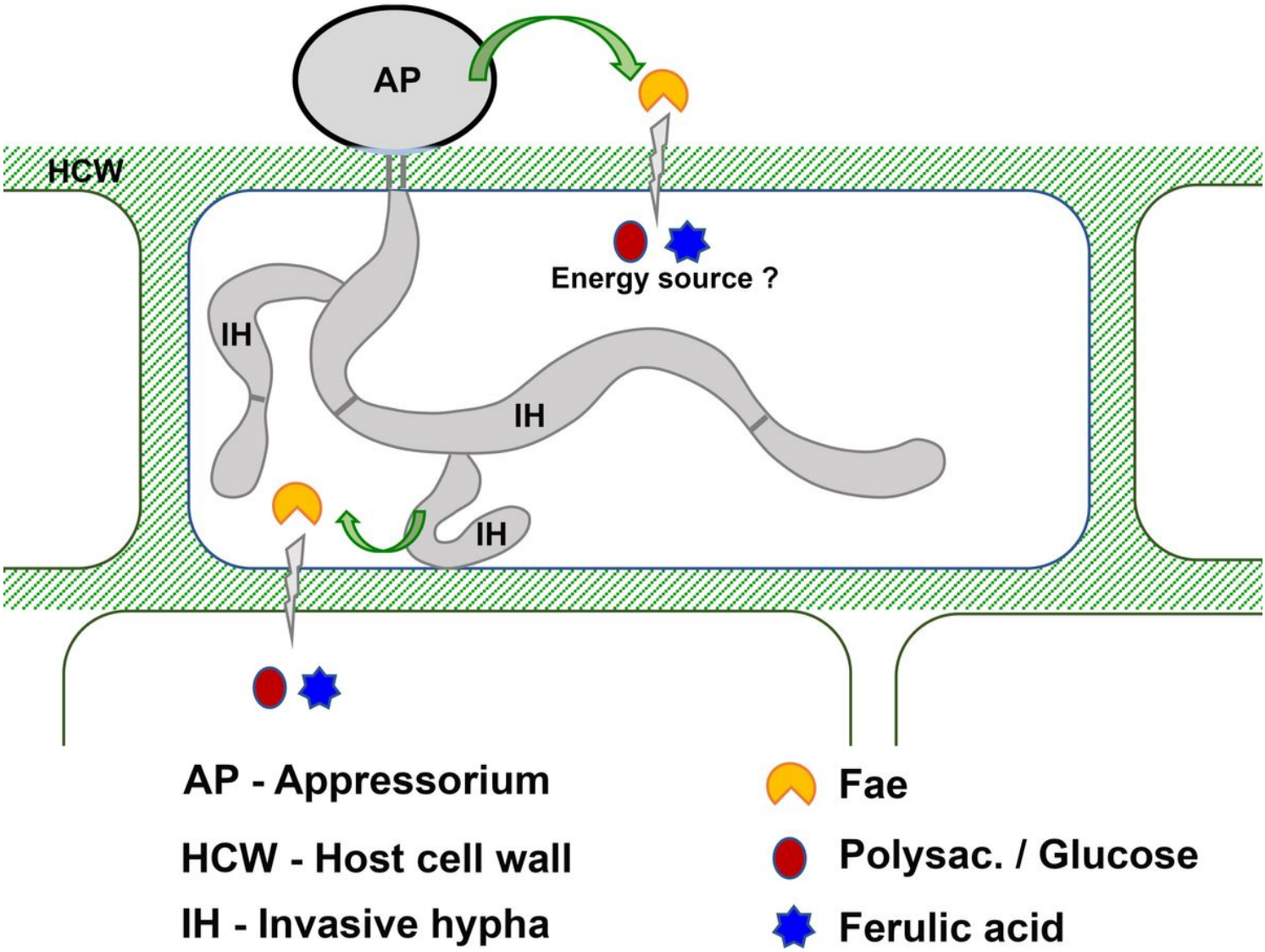

Figure 7

A proposed model of Fae1 function during pathogenesis in M. oryzae. Fae1, likely secreted along with other CWDEs, hydrolyses the plant cell wall to release ferulic acid and constituent carbohydrates during penetration of the first host cell and subsequent spread to the neighbouring cells. Released ferulic acid, the product of Fae enzyme action, and/or glucose, the breakdown product of cellulose, likely act as an energy source enabling successful host-invasion and colonisation by the blast fungal pathogen.

Supplementary Files

This is a list of supplementary files associated with this preprint. Click to download.

- SupplementaryInformationThakeretal.pdf